

## Influence of Geometric Simplifications on High-Intensity Radiated Field Simulations

Guadalupe G. Gutierrez<sup>1, \*</sup>, Sergio F. Romero<sup>2</sup>, Monica Gonzaga<sup>3</sup>, Enrique Pascual-Gil<sup>1</sup>, Luis D. Angulo<sup>4</sup>, Miguel R. Cabello<sup>4</sup>, and Salvador G. Garcia<sup>4</sup>

**Abstract**—This paper analyzes the influence of simplifications in electromagnetic models used in the design of protections against High-Intensity Radiated Field (HIRF) threats. Both conductive and radiated effects are evaluated, covering the wide frequency range between 1 MHz and 6 GHz. A real and complex test case such as the power plant of an A400M aircraft was simulated using FDTD method so as to analyse the impact of different simplification approaches. The parameters studied are the inclusion/removal of installations, modification of electrical contacts, material properties, and changes in the cable features. In consequence, we can conclude that for the frequency range around tens or hundreds of megahertz every detail is important (all the pieces of the model, accurate bundle routes and cable properties), while for higher frequencies only the details nearby the analyzed point are relevant for the results and it is not necessary to distinguish between different materials which are good conductors at this frequency range.

### 1. INTRODUCTION

The increment in the use of electronics and complexity in modern aircrafts, and the expanded use of the spectrum worldwide make the topic of susceptibility under High-Intensity Radiated Field (HIRF) conditions a key issue for the certification of any air vehicle. The frequency spectrum of HIRF threats ranges from 10 kHz to 40 GHz. Roughly speaking, below 400 MHz, the dominant effect comes from the excitation of airframe resonances, which induces currents on the cable bundles of the aircraft. The penetration of the electric field into the equipment bays via gaps, seams, radiofrequency transparent materials, and apertures in the airframe structure and equipment enclosures has an increasing influence above 100 MHz. This energy, coming from the bundles into the equipment in the first case, or electromagnetic (EM) fields at wavelengths comparable to the equipment sizes in the second one, interacts directly with the avionic systems, being a source of malfunctions [1]. In the present paper, both conductive and radiated effects are analyzed.

Three measurement techniques are commonly described by standards [2] so as to certify an aircraft in an HIRF environment: Low Level Direct Drive (LLDD), Low Level Swept Current (LLSC) and Low Level Swept Fields (LLSF). LLDD consists of a low level Direct Current Injection (DCI) whose objective is to relate the currents induced into the harnesses due to an applied external field by relating, in a first step, the currents induced into the harnesses with the surface current densities excited in the aircraft skin by measurements, and, in a second step, the surface current densities excited in the aircraft skin with the applied external field by simulations. This technique is used from 10 kHz up to 2 MHz (or up to the first resonant frequency of the aircraft, to have an overlap region) due to the impossibility of having a good radiating antenna at this lower frequency range. For LLSC, applied from 2 to 400 MHz,

---

*Received 27 June 2018, Accepted 24 August 2018, Scheduled 5 September 2018*

\* Corresponding author: Guadalupe Gutierrez Gutierrez (Guadalupe.Gutierrez@airbus.com).

<sup>1</sup> Airbus Defence and Space, Getafe, Spain. <sup>2</sup> INTA, Torrejon de Ardoz, Spain. <sup>3</sup> CT Ingenieros, Getafe, Spain. <sup>4</sup> Department of Electromagnetism, University of Granada, Granada, Spain.

the aircraft is situated on a metallic ground plane and is radiated by an antenna with a low level EM field from different directions and polarizations, and the induced currents in the cables connecting the equipment are measured so as to determine a transfer function between the illuminating EM fields and the induced currents. Similarly, above 100 MHz, the aircraft is also radiated and LLSF technique is used instead to relate the internal HIRF environment at the location of the relevant electric or electronic systems with respect to the external HIRF threat.

EM models and numerical codes are useful and powerful tools which can predict the electromagnetic performance and carry out parametrical studies during the design phase, when changes are simpler and less costly. In the following phases (certification, maintenance etc.), time of aircraft testing can be saved using simulations to perform this kind of analysis. When generating a 3D EM model of an electrically-large and complex object, a geometry simplification is needed in order to represent the reality in an easy to use model in terms of both size and complexity. Therefore, it is important to know which features may have an effect and which ones can be neglected. To this end, geometrical simplifications are intended to reduce the complexity of the model without degrading the simulation results [3, 4]. In this paper, the sensitivity of simulation results to variations of the model is analyzed to identify unnecessary elements for the simulations while retaining the essential physics of the problem. This study is focused on HIRF and, therefore, results obtained from simulations must be post-processed following the procedure established in the international HIRF regulations [2].

In this way, the present study aims to extend the analysis made in [5] for lightning indirect effects (LIE) to the simulations under a HIRF environment. This study is focused on frequencies from 1 MHz to 6 GHz. This frequency range covers LLSC and the first third of LLSF aircraft tests. Higher frequencies can be simulated at aircraft level by means of other methods [6, 7]. Frequencies covering the range of LLDD aircraft test were analyzed in [5]. In fact, this previous study can be considered valid for a frequency spectrum up to around 50 MHz.

A numerical model of the power plant (PWP) of the A400M aircraft [8] is employed to assess which parameters are most influential in an EM simulation, by conducting an heuristic approach based on a computationally affordable set of simulations. In particular, we study the importance of including or not all the systems and their installations, maintaining the electrical contacts, assigning different materials and selecting the relevant cables with their significant properties. We then estimate the sensitivity of these simulation results to variations in the EM model. This study let us provide theoretical guidelines together with a quantitative notion of the error magnitude which is made with these approximations. The factors which should be taken into account in a 3D EM model for HIRF are analyzed using this real and complex test case, so as to quantify their influence in the simulation results. Other factors are revealed as not important for this kind of simulations. The guidelines and conclusions presented in this paper can be extrapolated to other structures with the same level of complexity.

The rest of the paper is organized as follows. In Section 2, the model of the PWP is described, the features of the simulations performed are explained, and the pass/fail criterion established for this analysis is presented. Section 3 shows the results obtained and discusses the modifications taken into account, for both conductive and radiated effects. Finally, in Section 4, we draw the main conclusions of our analysis.

### 1.1. List of Acronyms

ACOC Air Cooled Oil Cooler	EVIS Electronic Vibration Isolation System
BPSV Bleed Pressure Regulator Shut-Off Valve	FDTD Finite Difference Time Domain
CAD Computer-Aided Design	FW Firewall
CFC Carbon Fiber Composite	HIRF High Intensity Radiated Field
CFL Courant-Friedrichs-Lewy	HPSV High Pressure Shut-Off Valve
DCI Direct Current Injection	IPSA Inlet Particle Separator Actuator
DFT Discrete Fourier Transform	LIE Lightning Indirect Effects
ECU Electronic Control Unit	LLDD Low Level Direct Drive
EM Electromagnetic	LLSC Low Level Swept Current
EMC Electromagnetic Compatibility	LLSF Low Level Swept Fields
EPB Electrical Propeller Brake	MTLN Multiconductor Transmission Line Network
EPMU Engine Protection and Monitoring Unit	OILS Oil System

PBCU Propeller Brake Control Unit  
 PCI PreCooler Installation  
 PCU Propeller Control Unit  
 PEC Perfect Electric Conductor

PML Perfect Matching Layer  
 PWP Power Plant  
 SCU Stationary Control Unit

## 2. ROADMAP

### 2.1. Model Details

The EM model of the A400M PWP represented in Fig. 1 was selected for our parametric study for two main reasons: it is a complex model fully representative of the complexity of a real aircraft which allows us to perform most of the modifications needed for this study, and its size is computationally affordable so that a large number of simulations can be performed. The PWP has three main structural components: the engine, the mounting and the nacelle. The engine and the mounting are mainly composed of metallic structures. The nacelle includes the fairings, which are mostly made of carbon fibre composite (CFC). For the reference model used in our comparisons, all the equipment and installations are included. The total length of the PWP is around 6 m.

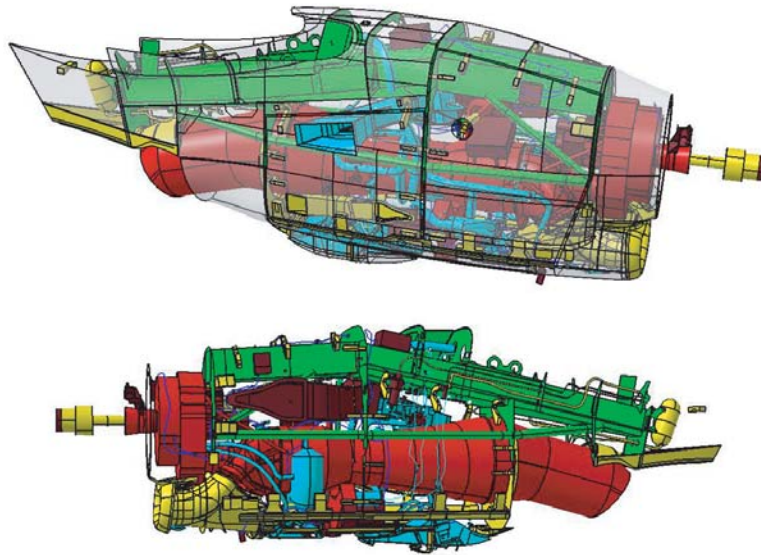


**Figure 1.** A400M PWP EM model (carbon fibre nacelle shown in white with a degree of transparency; the metallic nacelle is in yellow, the mounting is in green, the engine is in red, the equipment is in brown, the systems are in cyan and the harnesses are in dark blue).

For conductive effects, four overbraided harnesses were included in the model to analyse the currents induced on them. They were especially selected between the real harnesses of the PWP to cover the different zones of the model (see Fig. 2). Their description is as follows:

- The Controller Area Network bus (CANBUS) harness has 16 branches that interconnect 10 items of equipment around the engine and another branch separated from the rest of CANBUS branches by the firewall, with sizes from 300 to 1500 mm.
- The Electronic Control Unit (ECU) and the Air Cooled Oil Cooler (ACOC) Actuator are connected through the ECU-ACOC harness. This is a simple cable with no branches, about 4 m long.
- The H502 harness connects two fire detection sensors located in the nacelle and extends 6 m across the lower fairing, with no branches.

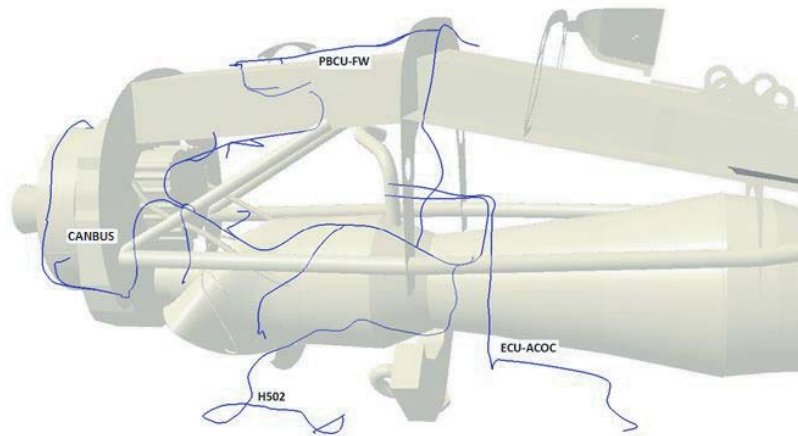


**Figure 2.** Conductive effects cable routes (left view) (the nacelle is not shown in the figure and the inner structure is depicted with a degree of transparency so that the complete routing of the cables can be seen).

- PBCU-FW is a harness with 7 branches, measuring no more than 600 mm, located between the mounting and the upper fairing. It connects the Propeller Brake Control Unit (PBCU) with the firewall (FW) to the wing.

The current induced at each cable branch was obtained from the simulations. Therefore, there are a total of 29 observables: 18 from CANBUS harness (among them, CANBUS-17 and CANBUS-18 are 2 probes located at each end of the CANBUS branch which is separated from the rest), 2 from ECU-ACOC (1 at each end), 2 from H502 (1 at each end) and 7 from PBCU-FW harness. These probes measure the current at particular thin wire nodes [9]. As it is usual in electromagnetic compatibility (EMC) testing, current probes were placed at a distance of 50 mm from the harness end for ending branches [10], and in the middle of the branch for the intermediate branches.

For radiated effects, equipment and cables were not included in the model since the observable is the electric field at the equipment location. The electric field at the location of the main items of equipment of the PWP was obtained from the simulations. A total of 12 equipment positions were analyzed, named by their equipment acronym (see Fig. 3 and Fig. 4). The average field for 8 probes distributed in their respective volumes was considered as the field at each equipment position.

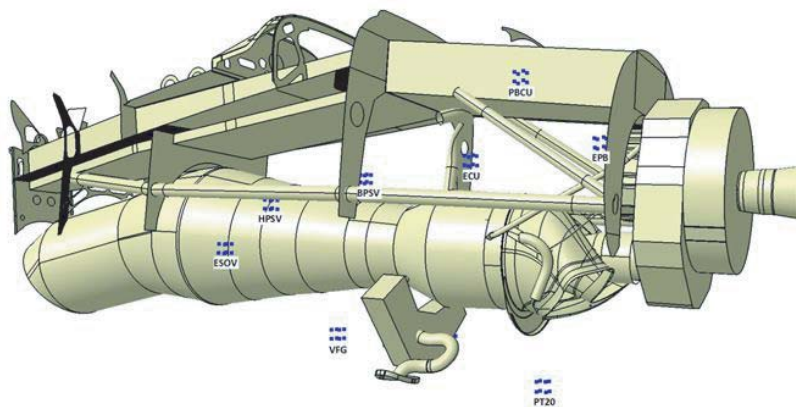


**Figure 3.** Radiated effects probes (right view) (the nacelle is not shown in the figure; items of equipment shown in this right view are located in different positions around the engine and even at the right side of the mounting).

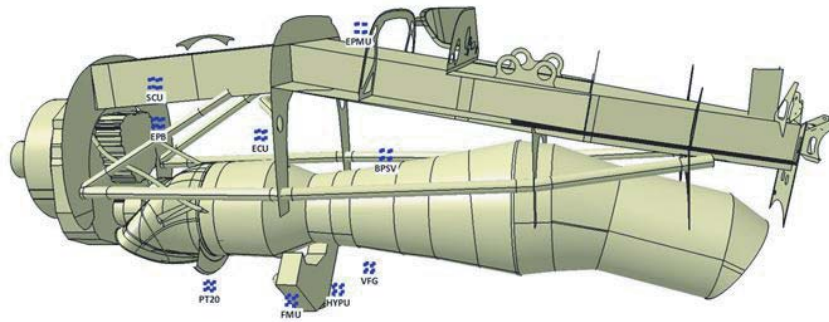


**Figure 4.** Radiated effects probes (left view) (the nacelle is not shown in the figure; items of equipment shown in this left view are located in different positions around the engine and even at left side and above the mounting).

## 2.2. Simulation Description

The previously described EM model was meshed in a Cartesian grid, suitable for Finite Difference Time Domain (FDTD), with a constant space-step of 5 mm, which corresponds to 10 samples per wavelength at the maximum frequency of 6 GHz. Perfect Matching Layer (PML) absorbing boundary conditions were employed to truncate the domain [11], yielding a problem size of around 700 Mcells. A time-step of 6 ps was employed to meet the Courant-Friedrichs-Lewy (CFL) stability condition [11]. A total time of 10  $\mu$ s was simulated, which was sufficient to have a fair convergence of the currents. A computation time of approximately 15 days, using 4 Intel Xeon eight-core 2.9 GHz nodes with 128 GB of memory (speeding up to 900 Mcells/s), was required for each configuration.

HIRF effects should be analyzed from 10 kHz to 18 GHz. Below 100 MHz the main coupling mechanism is that interconnecting wires act as receiving antennas, while above 400 MHz the primary contribution is due to field penetration through apertures. Between 100 MHz and 400 MHz, the dominant coupling mechanism is not clear and both current and field data should be considered. However, as explained in [12], even above 400 MHz, coupling occurs not only through physical openings directly into the electrical or electronic equipment but also through the interconnecting wiring within roughly a wavelength of distance from the connector on the aircraft equipment. Therefore, in the present study, conductive effects were analyzed from 1 MHz up to 1 GHz, whereas radiated effects were analyzed from 100 MHz up to 6 GHz. No data was collected from 10 kHz up to 1 MHz, since a huge calculation time would be necessary to attain convergence and it is out of the resonance zone. In addition, as it was said before, frequency range below 50 MHz was analyzed, both in time and in frequency domains, for LIE in [5]. For the maximum frequency, studying up to 6 GHz was considered a good compromise between the necessary computational resources and the interest of the obtained results.

The illumination from the antennas used in the experimental setup can be replaced computationally by plane waves, with a Gaussian waveform covering the spectral range up to 6 GHz. Several combinations of plane wave orientation and polarization were compared for reference configuration (complete model). Illumination from the right side and with horizontal polarization was considered the worst case for the majority of cases. The present study was focused on this particular illumination condition since conclusions can be extended to any other incidence.

## 2.3. Simulation Tools

Several EM simulation tools can be used in the design of protection against HIRF. Among them, as already mentioned, we selected one based on the FDTD technique [11] as the most suitable method for this kind of problem, as it obtains the solution in the whole frequency range with a single execution. In this study, the 3D computer-aided design (CAD) CATIA V5 R21 [13], the FDTD mesher CADfix V8.1 SP2.0 64bit [14], and the FDTD solver UGRFDTD R2660 [15] were used to generate the simplified CAD, to mesh it and to simulate it, respectively.

CADfix allows the user to mesh the region where EM propagation is to be calculated. It serves

as a graphical user interface which can import data from CAD models. All relevant EM properties (permittivity, permeability, impedance, etc.) can be defined, together with the boundary conditions, mesh density, probe locations, etc.. CADfix generates a text file containing all the information needed to specify the problem, and this can provide the input to UGRFDTD. This solver is a state-of-the-art parallel 3D full-wave EM simulation tool which uses the FDTD method [11,16], combined with a multiconductor transmission line network (MTLN) solver [17] to address the cabling. It was developed by UGR in collaboration with Airbus Defence and Space within several research and technology projects [18,19]. It is especially suited to deal with HIRF/Lightning electrically-large EMC problems [7, 20–23], and can account for complex structures, materials, cables, composite thin-panels, etc.. Further information about thin-panel and thin-wire formulation can be found in [24, 25] and [9, 17, 26] respectively. A variety of output data can be obtained including the electric current and voltage transient profiles stressing electric/electronic equipment considered in this study.

#### 2.4. Post-Process and Pass/Fail Criterion

For conductive effects, the current induced at each cable branch was collected in time domain and the Discrete Fourier Transform (DFT) was applied to them. Then, the octave enveloping method defined in [2] was applied, consisting in setting the peak current value constant for all the frequencies that are one octave lower and higher than the frequency of each peak. The results in dB( $\mu$ A) were depicted. Later, the difference between the octave envelope obtained from the modified configuration (model variation under study) and the reference one (complete model) was calculated and represented in dB

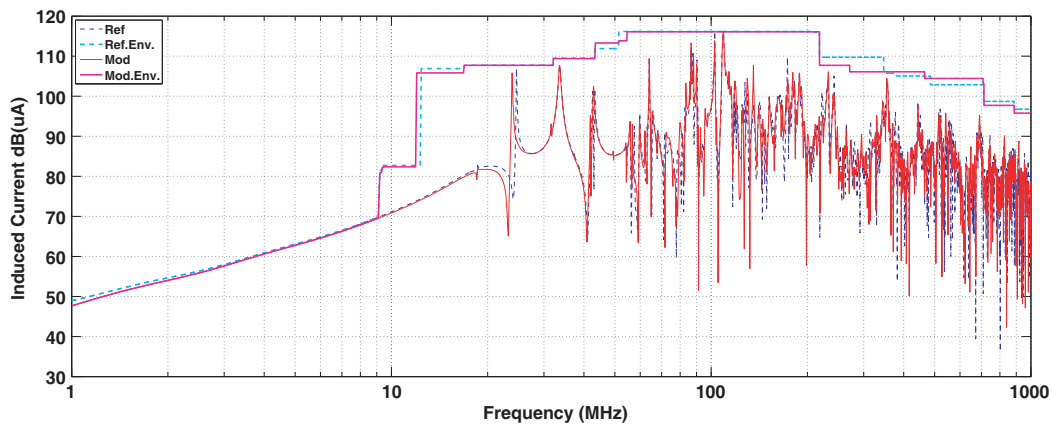


Figure 5. Raw data and octave envelope (affected cable).

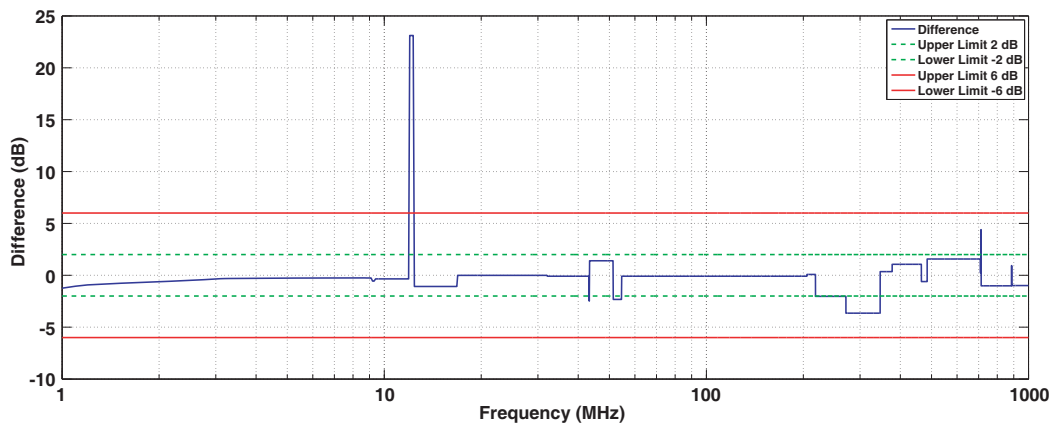


Figure 6. Difference and limits (affected cable).

along with the selected margins in order to analyse impact of each particular modification. Usually, the margin of HIRF simulations is 6 dB. This margin accounts not only for EM model precision but also for other uncertainties such as tolerances or numerical errors. Let's take a difference of 2 dB (approximately 25% error) to classify unaffected and affected cables. The limit of 6 dB will separate affected from highly affected cables.

Figure 5 and Figure 6 show the data processing applied to a cable affected by a particular modification in the EM model as an example of the followed post-process. In these graphs and the following ones, Ref. stands for the reference model (complete model) while Mod. for the modified one, and Env. stands for the octave or the 10% sliding frequency window (described below) envelopes while Avr. for the 5% averaging defined in [2]. As can be seen, between 50 and 60 MHz and between 200 and 400 MHz, the difference between modified and reference configurations for two short frequency ranges is higher than 2 dB, which means that it is an affected cable. Narrower deviations, such as the ones around 12, 43 and 711 MHz, are neglected since they do not represent a high difference in amplitude but an small shift between peaks, what is tried to be eliminated by the octave enveloping. This neglected peak is especially prominent for most of the cables between 10 and 20 MHz due to the first resonance peak.

Figure 7 and Figure 8 show the data processing applied to a cable unaffected by a modification. This cable was considered unaffected since the difference is maintained below  $\pm 2$  dB except for very narrow frequency ranges which, as explained before, were neglected. It should be noted that differences between modified and reference configuration at high frequency are less important than differences at

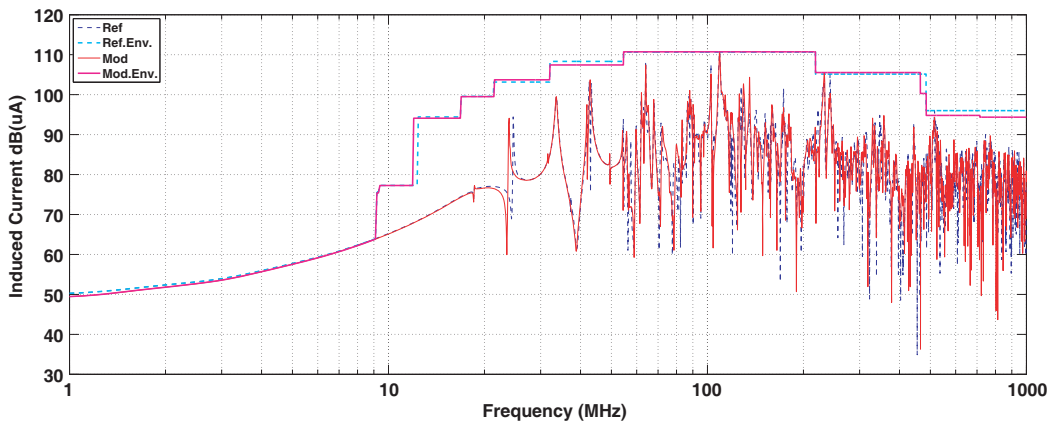


Figure 7. Raw data and octave envelope (unaffected cable).

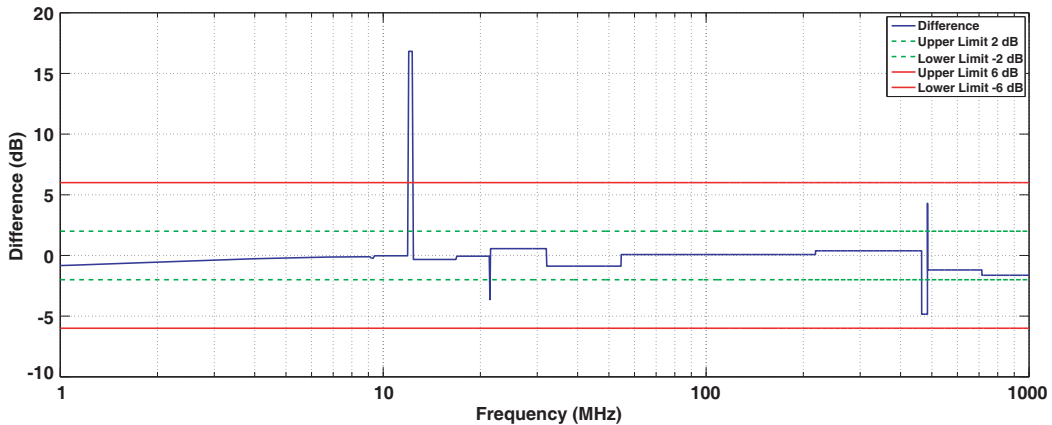


Figure 8. Difference and limits (unaffected cable).

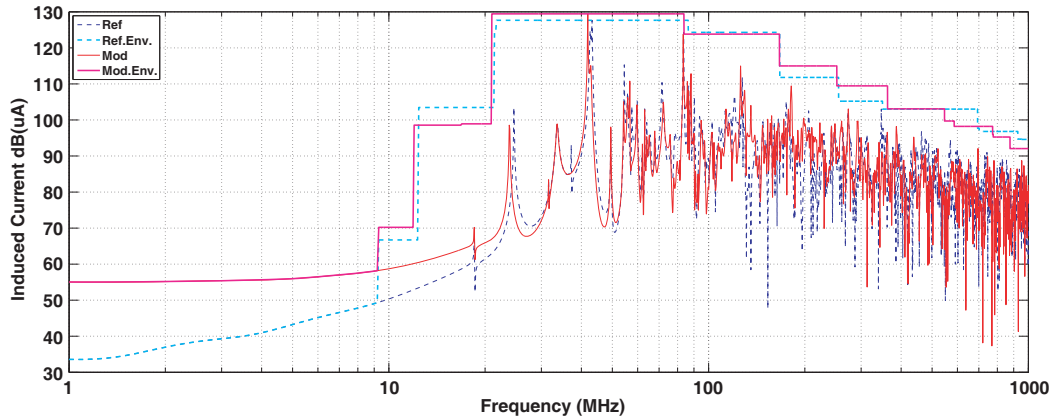


Figure 9. Raw data and octave envelope (highly affected cable).

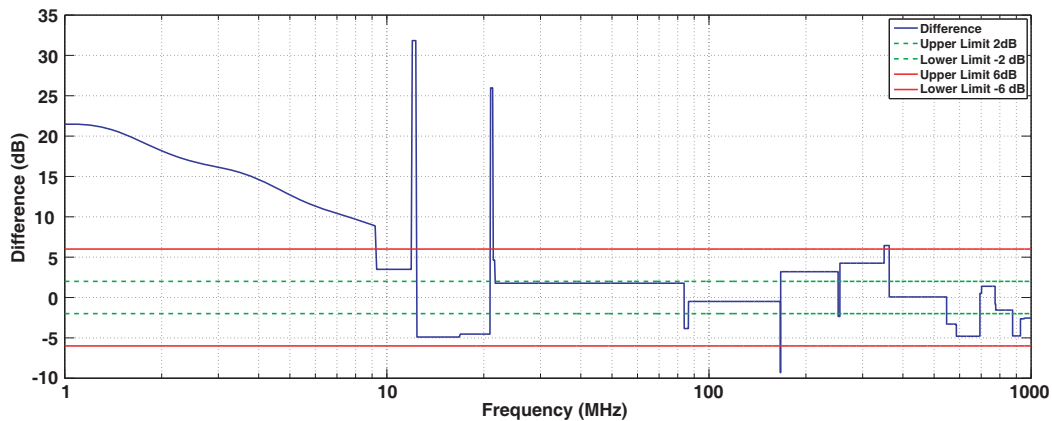


Figure 10. Difference and limits (highly affected cable).

low frequency. The reason is that from 400 MHz, or even from 100 MHz, the octave enveloping applied could be substituted for an envelope within a sliding frequency window of 10% [2], which would lead to narrower and smaller differences.

Figure 9 and Figure 10 show the data processing applied to a cable highly affected by a modification. As can be seen, the difference is higher than 6 dB, especially for low frequencies, and higher than 2 dB in many other frequencies.

For radiated effects, the three cartesian components of the  $E$  field at eight points inside the volume of the equipment under study were collected in time domain. Those internal fields were Fourier transformed to perform the required operations. Then, the total field at each point was calculated and the mean value from the eight points inside each item of equipment was used to carry out the comparisons. After that, the averaging of the linear values in a 5% bandwidth and the enveloping within a sliding frequency window of 10% of any given frequency defined in were applied [2]. Finally, the results in dB(V/m) were depicted and the difference between modified and reference configurations along with the  $+/- 2$  and  $+/- 6$  dB limits were represented as well.

Figure 11 and Figure 12 show the data processing applied to a field probe as an example of the followed post-process for an item of equipment highly affected by removing the systems. This position is near to PreCooler Installation (PCI) system. In the configuration without systems, the  $E$  field level at this position for low frequencies diminishes a lot. It seems that PCI introduces field inside the PWP and, therefore, more field level is found at those locations at the center of the volume. Removing the PCI (without systems), the field which enters through the PCI aperture is more uniformly distributed and constant with the frequency.

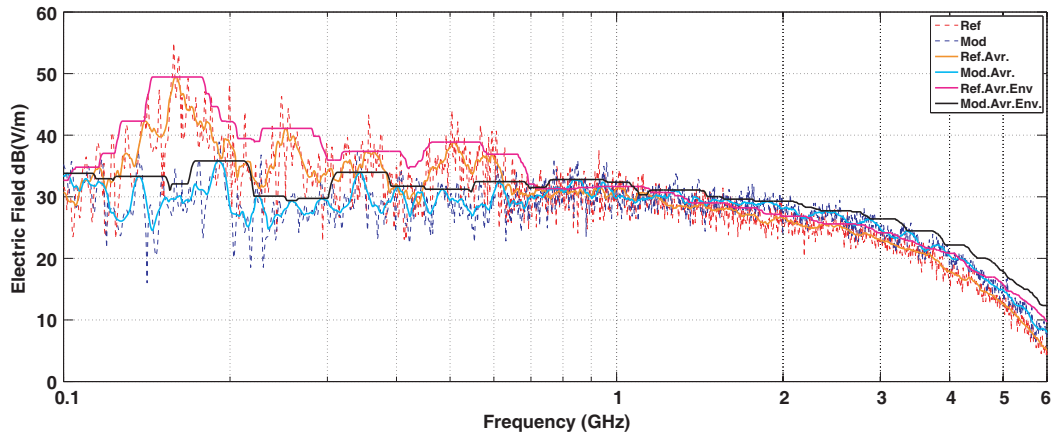


Figure 11. Raw data and envelopes (highly affected equipment).

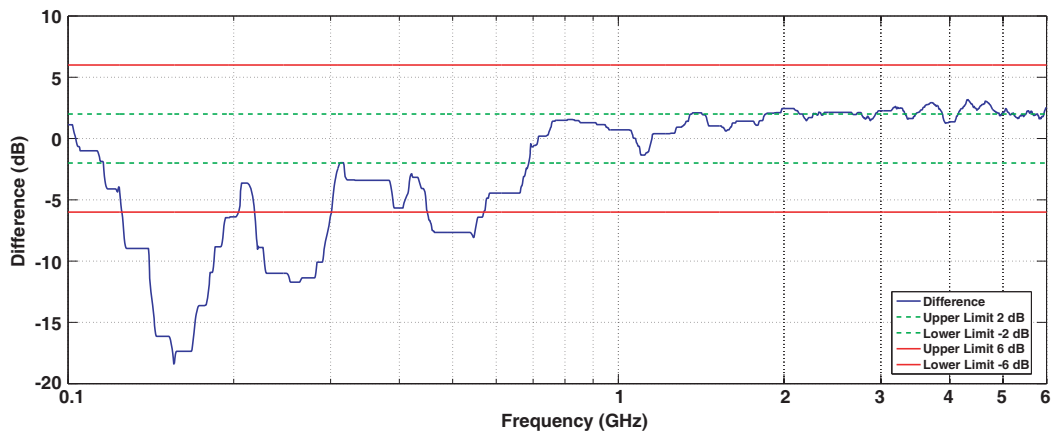


Figure 12. Difference and limits (highly affected equipment).

### 3. ANALYSIS OF RESULTS

#### 3.1. Conductive Effects

Several configurations belonging to four different kinds of tests were analyzed in order to quantify the importance of: including the surrounding installations, maintaining all the electrical contacts, assigning different materials and selecting the relevant cables with their significant properties.

Table 1 shows the summary of the results for conductive effects. Frequencies from 1 MHz to 1 GHz were analyzed. The first column indicates the modification analyzed in each row. Columns two, three and four give the number of cables which have been unaffected, affected or highly affected respectively by each modification in the EM model. A figure of merit referred to as factor is shown in column five to quantify the impact of each modification. This factor was calculated by adding the number of unaffected cables multiplied by one, the number of affected cables multiplied by two and the number of highly affected cables multiplied by three. The modifications of greater impact have the factor cell coloured in red (factors higher than 52, which could mean that half of the cables are unaffected, and, among the affected cables, one half is only affected and the other half is highly affected), the ones with lower impact in yellow (factors between 30 and 51) and the ones with no impact in green (factor = 29). The last column is used for indicating the width of the frequency ranges with differences beyond the limits (*S* stands for small, which is a deviation in approximately less than 25% of the frequency range of interest; *M* for medium, which is a deviation in approximately between 25% and 50% of the frequencies;

**Table 1.** Conductive effects.

MODIFICATION	UNAFF <sup>1</sup>	AFF <sup>1</sup>	HIGHLY AFF <sup>1</sup>	FACTOR	FREQ. RANGE
Without OILS	1	18	10	67	S-LH
Without IPSA	0	8	21	79	S-LH
Without Systems	0	5	24	82	M-LMH
With EVIS	0	6	23	81	M-LMH
Without PCU Connection	2	6	21	77	M-LM
PEC	17	4	8	49	M-LMH
Cable Displacement	0	0	2(/2)	6 <sup>2</sup>	L-LMH
Without Ramifications	0	0	11(/11)	33 <sup>2</sup>	L-LMH
$R_c = 10 \text{ m}\Omega$ , $R/l = 10 \text{ m}\Omega/\text{m}$	29	0	0	29	n/a
$R_c = 100 \Omega$	0	0	29	87	L-LMH
Pig-tail termination	0	8	21	79	S-H
Reduced Radius 40%	0	19	10	68	S-H
Reduced Radius 80%	0	9	20	78	M-LMH

<sup>1</sup> AFF stands for AFFECTED. Difference values beyond the limits at very narrow frequency ranges were neglected.

<sup>2</sup> Factor cell of Cable Displacement modification is coloured in red even though the factor is only 6 because the number of cables potentially affected by this modification is 2. Similarly, factor cell of Without Ramifications modification is coloured in red even though the factor is only 33 because the number of cables potentially affected by this modification is 11.

and  $L$  for large, which is a deviation in approximately more than 50% of the frequencies) and for which frequencies the differences are beyond the limits ( $L$  stands for the lower decade,  $M$  for the medium decade, and  $H$  for the higher decade). For instance, Figs. 5 and 6 correspond to the configuration without Oil System (OILS) and show that the cable is affected in a small-sized frequency range at mainly high frequencies (S-H) (this configuration is assessed as S-LH because other cables are affected for the low frequency range).

### 3.1.1. Removal of Components

Since geometric simplification is extremely time consuming when a complex geometry is to be simplified, it is important to know which components (equipment, systems, installations, etc.) are relevant for the model. The first group of modifications try to give some clues about this issue.

*Removal of OILS.* Firstly, we analyze what happens if we remove the OILS from A400M PWP model. OILS is a system located in the lower fairing, far from the majority of the cable branches but in electrical contact with ECU-ACOC harness (see Fig. 13).

The factor shown in Table 1 for this modification means that removing OILS entails a considerable variation in the currents induced by a HIRF threat. Even far cables are affected, because, up to frequencies of hundreds of MHz, modifications at a distance of meters can alter the results.

*Removal of Inlet Particle Separator Actuator (IPSA).* The same conclusions as in the previous section can be drawn even removing an small item of equipment (see IPSA in Fig. 13). In this case, even more cables are affected and the variations encountered are bigger.

*Removal of all systems.* Now, let's see what happens if we remove, not only OILS and IPSA, but all the systems from the model (dark blue pieces in Fig. 13). For the cables terminating at a system, we created a fictitious connection to the nearest perfect electric conductor (PEC) structure in order to degrade as little as possible the cable ends.

As shown in Table 1, this is one of the modifications which more affects the results in amplitude of the differences, in the shape of the curves and in the trend at low frequency. In the example of Fig. 14 can be clearly seen that the prediction without systems undervalues the results for many frequencies,

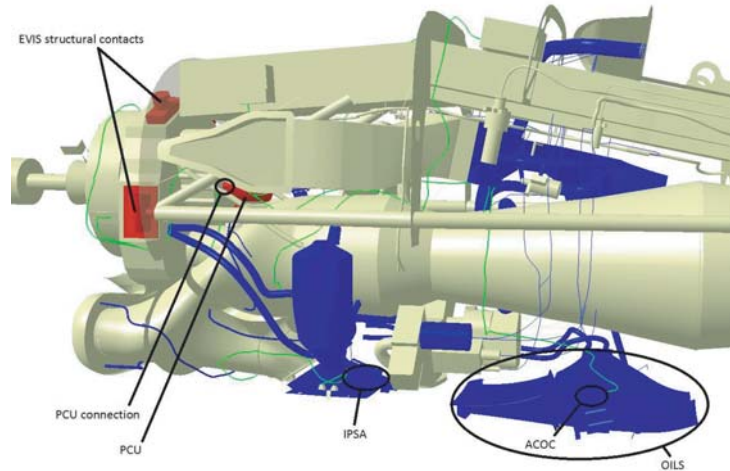


**Figure 13.** Detailed view of the EM model (some parts not shown or depicted with a degree of transparency to visualise the inner structure; systems are in dark blue and harnesses in green).

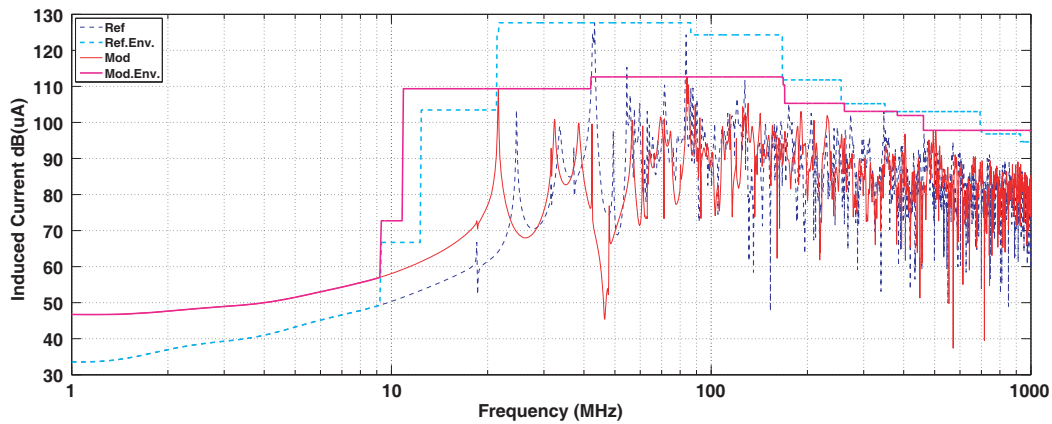


**Figure 14.** Raw data and octave envelope (removal of all systems — conductive effects).

which would lead to a risk in a qualification/certification process.

It is worth noting that the first resonance peaks in the induced currents belong to structure dimensions (23 MHz is half a wavelength of the object electrical length), whereas higher resonance peaks correspond to cable branches' length (between 0.3 and 6 m).

### 3.1.2. Change of Electrical Contacts

The following two examples highlight the importance of correctly modelling the electrical contact between different components.

*With the Electronic Vibration Isolation System (EVIS) structural contact.* In this section we would like to evaluate how affects the results the error of introducing a piece in the EM model as conductor instead of as lossy or even insulating material. Unless we have a really full mock-up with data about materials and even composing materials of every piece, it is logic to suppose that two pieces with mechanic contact between them are also in electrical contact, but that is not the case when non conductor materials are involved.

In order to demonstrate that this mistake can be important, we chose the four EVIS of the A400M PWP, which connect the engine with the mounting at the front part of the model, but are insulating (see Fig. 13). The electrical connection is guaranteed by four bonding jumpers because the current

should pass from the engine to the mounting.

In the light of the results presented in Table 1 the effect of this modification is similar to the effect of removing the systems. In fact, this case could be included in the group called removing elements, since in HIRF problems we have an EM wave impinging on the structure and not a current injection where the most important issue are the electrical contacts. The inclusion or the lack of EVIS changes the field distribution and, as a consequence, the induced currents.

This modification affects the results in amplitude of the differences, in the shape of the curves and in the trend at low frequency.

*Without Propeller Control Unit (PCU) connection.* The PCU is an item of equipment which is joined to the engine by a set of cylinders (see Fig. 13) opened by different zones of the digital mock-up (mock-ups are usually divided into zones so that it is not necessary to open in the CAD program the complete model to see one particular thing, with the resulting saving of memory).

Table 1 shows how many cables are affected if the modeler forgets to include in the model only one of those tiny cylinders, which could happen when the zone that opens it is not present on the screen.

Removing PCU connection leads to a new resonance around 26 MHz. Moreover, the induced current is higher even for the cable branch connected to the PCU (up to 50 dB( $\mu$ A)), which would be disconnected in this configuration. Even other harnesses not connected to the PCU can be affected, but only at low or at the new resonance frequencies and with low levels compared with the maximum levels for those cables.

### 3.1.3. Inclusion of Non-PEC Materials

The configuration presented right after was devised to analyse the importance of considering materials other than PEC in HIRF simulations.

*PEC.* The most part of the nacelle is made of CFC and it was modeled in FDTD with the sub-cell model described in [24, 25]. In the present study mean values of conductivity and thickness for the thin-layer material were assigned and no anisotropy was taken into account (conductivity of  $2.2 \times 10^4$  S/m and 2 mm of thickness for CFC and conductivity of  $3.3 \times 10^4$  S/m and 2 mm of thickness for CFC with bronze mesh). Table 1 shows that modelling it as PEC is a factor of low impact. Moreover, although there are highly affected cables, it is not due to different levels but to a lack of convergence in the case of PEC. The EM model used for this study does not include lossy materials, such as internal coating, that would absorb the energy, and, therefore, the energy is more time bouncing inside the volume. On one hand, this fact affects the DFT performed to analyse the results in the sense that more simulation time would be necessary to attain fully converged results in the low frequency range. On the other hand, some different resonances could be obtained as a consequence of these bounces.

### 3.1.4. Cable Properties and Modifications

This forth group of modifications is used to study the influence of the cable properties such as their route, impedance or radius on an EM model.

*Cable displacement.* CANBUS-17 is a point to point cable which runs from the firewall to the Engine Protection and Monitoring Unit (EPMU). It is separated by the firewall from the rest of CANBUS branches. This short cable was displaced around 10 cm from its original route. Table 1 shows how this modification highly affects the results (note that only two probes are applicable).

*Suppression of Ramifications.* In this section we analyse the impact of introducing into the EM model all the cable branches in a HIRF simulation. Branches other than the ones going from PBCU to firewall connectors through both CANBUS and PBCU-FW harnesses were disregarded.

Table 1 shows how this modification highly affects the results up to 500 MHz (note that only eleven probes are applicable) in amplitude of the differences, in the shape of the curves and in the trend at low frequency.

*Connector resistance and resistance per unit length.* Typically, the first simulations are performed during the design process, and, therefore, with generic values for over braid resistances, since their real value is unknown at these early steps. It makes sense, thus, to wonder if simulations should be repeated with real over braid resistances when they are known. In order to answer this question, we duplicated the

connector resistance (from 5 to 10 mΩ) and over braid resistance per unit length (from 5 to 10 mΩ/m), which would be a reasonable variation between generic and real values. As shown in Table 1, all the cables are unaffected by these modification. Only very short cables can reflect any variation due to their connector resistances

*Equipment isolation or high resistance internal circuit.* By contrast, if the items of equipment are isolated or the internal circuits at each pin have high resistances (in common mode, that is, with respect to the equipment chassis), the induced currents are completely different (see Table 1 for a change from 5 mΩ to 100 Ω), and therefore, those high resistances should be considered in the simulation. In general, current induction levels are lower in the whole frequency range (more than 20 dB(μA)), especially for the lower frequencies, but voltage values will be high.

*Pig-tail termination.* Due to their low inductance, 360 degrees connector backshells are typically used for grounding the shields. Nevertheless, pig-tails are utilized to ground the shields in some cases. For that reason, we analyzed the effect of those pig-tails in the induced currents. A pig-tail inductance of 100 nH was selected, which approximately corresponds to a pig-tail 10 cm in length and with a diameter of 1.5 mm. Table 1 shows the results. Important current variations are obtained, especially at high frequencies.

*Cable radii.* The MTLN approach of [17] is an extension of the classical Holland treatment of thin wires [9] which takes into account the coupling between parallel wires as well as that with the rest of the structure. In the Holland model, the radius of the cable impacts on the maximum time step for stability [26] and this should often be reduced in simulations in order to achieve a stable solution. In this section, we would like to analyse the viability of this measure. For that purpose, we diminished 40% and 80% the cable radius (from  $5 \times 10^{-4}$  m down to  $3 \times 10^{-4}$  m and  $1 \times 10^{-4}$  m, respectively). The results of these modifications can be seen in Table 1. The variation in the induced current is not so alarming for the 40% radius-reduction and affects mainly at high frequencies, but is really high for the 80% reduction and affects at the whole frequency range.

### 3.2. Radiated Effects

Three different configurations were compared with the reference case in order to quantify their importance. Table 2 shows the summary of the results for radiated effects. Frequencies from 100 MHz to 6 GHz were analyzed. As in the previous subsection, the first column indicates the modification analyzed in each row. Columns two, three and four give the number of cables which have been unaffected, affected or highly affected respectively by each modification in the EM model. The factor figure of merit shown in column five is used for quantifying the impact of each modification and was calculated by adding the number of unaffected positions multiplied by one, the number of affected positions multiplied by two and the number of highly affected positions multiplied by three. The modifications of greater impact have the factor cell coloured in red (factors higher than 21, which could mean that half of the positions are unaffected, and, among the affected positions, one half is only affected and the other half is highly affected), the ones with lower impact in yellow (factors between 13 and 20) and the ones with no impact in green (factor = 12). Similarly, the last column is used for indicating the width of the frequency ranges with differences beyond the limits and for which frequencies the differences are beyond the limits (here *L* stands for frequencies between 100 and 400 MHz, *M* between 400 MHz and 1.5 GHz, and *H* between 1.5 and 6 GHz). For instance, Figs. 11 and 12 correspond to the configuration without systems and show that the cable is affected in a medium-sized frequency range mostly spread over low and medium frequencies (M-LM).

**Table 2.** Radiated effects.

MODIFICATION	UNAFF <sup>1</sup>	AFF <sup>1</sup>	HIGHLY AFF <sup>1</sup>	FACTOR	FREQ. RANGE
Without Systems	0	5	7	31	M-LM
With EVIS	0	9	3	27	S-L
PEC	11	0	1	14	S-L

<sup>1</sup> AFF stands for AFFECTED

### 3.2.1. Removal of All Systems

Removing the systems of the EM model (go back to Section 3.1.1 to remind the modification description) varies a lot the results (see Table 2) in both the number of frequencies affected and the amplitude of the differences. Differences up to 40 dB(V/m) are found (see Fig. 15).

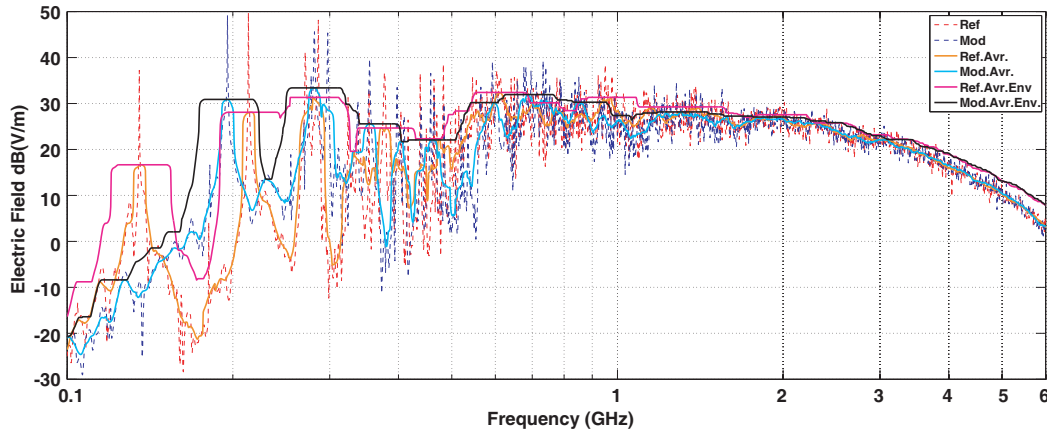


**Figure 15.** Raw data and envelopes (removal of all systems — radiated effects).

It is worth noting that the curves show how items of equipment such as EPMU or SCU are in well shielded zones (see Fig. 4), and have lower values of  $E$  field, while other items such as BPSV or HPSV (see Fig. 3) are more exposed to  $E$  field levels.

On the other hand, near the fairings, the cavity is resonant and the field presents many oscillations with the frequency. At the center volume, where there is room for air, the cavity is more like a reverberation chamber, and the field is much more uniform and constant with the frequency [27].

In general, for most of the positions, the field without systems should diminish, because the free volume is higher, and, therefore, the  $Q$  factor of the cavity and the field level are lower [27].

As can be seen in this section and the following ones, above 500 MHz, approximately where the PWP starts to work like a reverberation chamber, modifications have low impact. This starting frequency can be calculated using the Weyl formula (see [27]) which relates the cavity volume with the number of modes existing at a particular frequency. In our model, the volume is approximately  $8 \text{ m}^3$ , which leads to a starting reverberation frequency of around 300 MHz for an empty chamber. However, this frequency is delayed up to 500 MHz because the PWP is overloaded with equipment. The shielding effectiveness approaches to zero as the frequency increases. The modifications analyzed have effect mostly at the low frequency range, that is, from 100 up to 500 MHz, changing the firsts resonances in the areas where the equipment is located.

### 3.2.2. With EVIS Structural Contact

Table 2 shows the importance of this modification (go back to Section 3.1.2 to remind the modification description). The differences encountered are at the beginning of the band (frequencies lower than 500 MHz for the affected positions and lower than 200 MHz for the highly affected positions). The maximum difference is found for the EPB location and reaches 10 dB(V/m).

### 3.2.3. PEC

Table 2 shows that this modification (go back to Section 3.1.3 to remind the modification description) has low impact, and, even lower than that taking into account that the difference at the only position highly affected (7 dB(V/m)) is found at a minimum of the  $E$  field curves.

#### 4. CONCLUSIONS

The present study involves the execution of 20 different configurations, making a total of around 1600 analyzed signal-probes, being the computation time of each simulation approximately 15 days using 4 nodes with 128 GB of memory (900 Mcells/s). A statistical analysis is carried out with all these simulations to draw different conclusions.

The study is focused on frequencies from 1 MHz to 6 GHz, which covers LLSC and the first third of LLSF aircraft tests intended for HIRF certification. Typically, LLSC test is performed from 2 to 400 MHz and the transfer functions between the current induced in the aircraft wire bundles and the incident field are determined, while LLSF test is performed from 100 MHz to 18 GHz and determines the transfer functions between the internal bay fields and the incident field.

In the light of the results presented in the present document, we can conclude that LLSC covers the range more sensitive to any variation in the EM model because it is an intermediate frequency range and, as a consequence, is affected by induction, radiation, nearby objects, distant objects, etc.. Therefore, a complete and detailed EM model is a crucial point in order to obtain accurate LLSC results since, on one hand, the field distribution is strongly affected by the parts included in the model, and, on the other hand, the conductive effects also depends on cable properties. Resonances corresponding to both structure dimensions and cable lengths can be observed in the induced current curves.

Every piece should be included in the model, according to their material properties, because they can change the field distribution. It does not matter if they are in electrical contact with the cables under study or if they carry high currents, which are the most influential factors for the lower frequency range (below 50 MHz). In the intermediate frequency range (1 MHz–1 GHz), every piece is important.

Among cable properties, accurate bundle routes including all their ramifications properly bonded should be respected. Specific connector resistances should be considered provided that they are not of the same order than the generic values. Pig tail auto-inductance also changes the results. Cable radius can be reduced to get stability, within some limits, since 40% reduction causes not alarming but considerable changes.

At LLSF frequency range, as frequency increases, the field distribution is more homogeneous and only very close details can affect the results. The frequency behavior as a reverberation chamber can be related to the cavity volume according to Weyl formula. Besides, considering CFC material is not important at high frequencies since its properties are more and more similar to PEC ones with the increase in frequency.

#### ACKNOWLEDGMENT

This work has received funding from the Projects TEC2016-79214-C3-1-R, TEC2016-79214-C3-3-R, and TEC2015-68766-REDC (Spanish MINECO, EU FEDER), P12-TIC-1442 (J. de Andalucia, Spain), Alhambra-UGRFDTD (AIRBUS DS), and by the CSIRC alhambra.ugr.es supercomputing center.

#### REFERENCES

1. AC 20-158A, "The certification of aircraft electrical and electronic systems for operation in the high-intensity radiated fields (HIRF) environment," AIR-130, Aviation Safety — Aircraft Certification Service, Aircraft Engineering Division, May 2014.
2. EUROCAE ED-107, "Guide to certification of aircraft in a high-intensity radiated field (HIRF) environment," rev A, July 2010/SAE ARP 5583, rev A, June 2010.
3. Gil, E. P. and G. G. Gutierrez, "Simplification and cleaning of complex CAD models for EMC simulations," *International Symp. on Electromagnetic Compatibility EMC Europe*, York, UK, 2011.
4. Nogueira de Sao Jose, A., A. Colin, J. Fujioka Mologni, G. Maciulis Dip, U. do Carmo Resende, and S. Trindade Mordente Goncalves, "Computational savings based on three-dimensional automotive geometries' simplifications in electromagnetics simulations," *International Conference on Microwave and Optoelectronics*, Rio de Janeiro, 2013.
5. Gutierrez, G. G., S. F. Romero, M. Gonzaga, E. Pascual-Gil, L. D. Angulo, M. R. Cabello, and

- S. G. Garcia, "Influence of geometric simplifications on lightning strike simulations," *Progress In Electromagnetics Research C*, Vol. 83, 15–32, 2018.
6. Junqua, I., J.-P. Parmantier, and M. Ridet, "Modeling of high frequency coupling inside oversized structures by asymptotic and PWB methods," *Proc. Int. Conf. Electromagn. Adv. Appl. ICEAA*, 2011.
  7. Gutierrez, G. G., J. Alvarez, E. Pascual-Gil, M. Bandinelli, R. Guidi, V. Martorelli, M. F. Pantoja, M. R. Cabello, and S. G. Garcia, "HIRF virtual testing on the C-295 aircraft: On the application of a pass/fail criterion and the FSV method," *IEEE Trans. on Electromagnetic Compatibility*, Vol. 56, No. 4, 854–863, 2014.
  8. A400M, <http://militaryaircraft-airbusds.com/aircraft/a400m/a400mabout.aspx>.
  9. Holland, R. and L. Simpson, "Finite-difference analysis of EMP coupling to thin struts and wires," *IEEE Trans. on Electromagnetic Compatibility*, Vol. 23, No. 2, 88–97, 1981.
  10. RTCA/DO-160, "Environmental conditions and test procedures for airborne equipment," issue G, December 2010/EUROCAE ED-14, issue G, May 2011.
  11. Taflov, A. and S. Hagness, *Computational Electrodynamics: The Finite-Difference Time-Domain Method*, Artech House, 2005.
  12. RTCA/DO-307, "Aircraft design and certification for portable electronic device (PED) tolerance," issue A, December 2016.
  13. "CATIA by dassault systemes," <http://www.3ds.com>.
  14. "CADfix," <http://www.transcendata.com/products/cadfix/>.
  15. Garcia, S. G., J. Alvarez, L. D. Angulo, and M. R. Cabello, "UGRFDTD EM solver," <http://www.-sembahome.org/>, 2011.
  16. Yee, K. S., "Numerical solution of initial boundary value problems involving Maxwell's equations in isotropic media," *IEEE Trans. on Antennas and Propagation*, Vol. 14, No. 3, 302–307, 1966.
  17. Berenger, J.-P., "A multiwire formalism for the FDTD method," *IEEE Trans. on Electromagnetic Compatibility*, Vol. 42, No. 3, 257–264, 2000.
  18. "HIRF-SE project (2008)," <http://hirfse.axessim.eu/>.
  19. "Alhambra-UGRFDTD by CSIRC (2013)," <https://alhambra.ugr.es/>.
  20. Romero, S. F., G. G. Gutierrez, A. L. Morales, and M. A. Cancela, "Validation procedure of low level coupling tests on real aircraft structure," *International Symposium on Electromagnetic Compatibility EMC Europe*, 2012.
  21. Gutierrez, G. G., D. M. Romero, M. R. Cabello, E. Pascual-Gil, L. D. Angulo, and S. G. Garcia, "On the Design Of Aircraft Electrical Structure Networks," *IEEE Trans. on Electromagnetic Compatibility*, Vol. 2, No. 58, 401–408, 2016.
  22. Gutierrez, G. G., S. F. Romero, J. Alvarez, S. G. Garcia, and E. P. Gil, "On the use of FDTD for HIRF validation and certification," *Progress In Electromagnetics Research Letters*, Vol. 32, 145–156, 2012.
  23. Cabello, M. R., S. Fernandez, M. Pous, E. Pascual-Gil, L. D. Angulo, P. Lopez, P. J. Riu, G. G. Gutierrez, D. Mateos, D. Poyatos, M. Fernandez, J. Alvarez, M. F. Pantoja, M. A. Cancela, F. Silva, A. R. Bretones, R. Trallero, L. N. Fernandez, D. Escot, R. G. Martin, and S. G. Garcia, "SIVA UAV: A case study for the EMC analysis of composite air vehicles," *IEEE Trans. on Electromagnetic Compatibility*, Vol. 59, No. 4, 1103–1113, 2017.
  24. Sarto, M., "A new model for the FDTD analysis of the shielding performances of thin composite structures," *IEEE Trans. on Electromagnetic Compatibility*, Vol. 41, No. 4, 298–306, 1999.
  25. Cabello, M. R., L. D. Angulo, J. Alvarez, I. Flintoft, S. Bourke, J. Dawson, R. G. Martin, and S. G. Garcia, "A hybrid crank-nicolson FDTD subgridding boundary condition for lossy thin-layer modeling," *IEEE Trans. on Microwave Theory and Techniques*, Vol. 65, No. 5, 1397–1406, 2017.
  26. Schmidt, S. and G. Lazzi, "Use of the FDTD thin-strut formalism for biomedical telemetry coil designs," *IEEE Trans. on Microwave Theory and Techniques*, Vol. 52, No. 8, 1952–1956, 2004.
  27. Hill, D., *Electromagnetic Fields in Cavities: Deterministic and Statistical Theories*, IEEE Press, New York, 2009.